Another point which requires discussion is the systematic arrangement of peaks and valleys of residual electron density in the difference Fourier syntheses (Figs. 2 and 3). There are peaks of residual electron density approximately midway between the bonded carbon and nitrogen atoms, and valleys between the non-bonded carbon and nitrogen atoms of a molecule. These regions of residual electron density, both positive and negative, extend about 1 Å above and below the plane of the molecule. Integration of the residual electron density peaks, of the spherical refinement (Fig. 2), between the arbitrarily selected pairs of atoms C(3) and C(4), and C(5) and C(6) indicates that both of these regions contain approximately 0·1 electron in 1·3 Å^3. Application of the methods suggested by McWeeny (1951, 1952, 1953, 1954) for X-ray scattering by bonded atoms would probably eliminate many of the systematic peaks and valleys of the difference Fourier synthesis. Application of these methods would account for some of the scattering power in the bonds and would reduce the apparent thermal motion in the plane of the molecule. This reduction in the apparent thermal motion would tend to remove electrons from the non-bonded regions and eliminate the valleys of the difference Fourier.

The authors wish to thank D. T. Cromer, R. B. Roof, and Prof. K. N. Trueblood for their interest and discussions concerning this structure. Thanks are also due Mrs Lois Duncan for help in gathering the intensity data.

References

Busing, W. R. & Levy, H. A. (1964). *Acta Cryst.* **17**, 142.

Chao, G. Y. & McCullough, J. D. (1962). *Acta Cryst.* **15**, 887.

Cruickshank, D. W. J. (1949). *Acta Cryst.* **2**, 65.

Cruickshank, D. W. J. (1956*a*). *Acta Cryst.* **9**, 754.

Cruickshank, D. W. J. (1956*b*). *Acta Cryst.* **9**, 757.

Cruickshank, D. W. J. (1961). *Acta Cryst.* **14**, 896.

Evans, H. T., Jr. (1961). *Acta Cryst.* **14**, 689.

Forsyth, J. B. & Wells, M. (1959). *Acta Cryst.* **12**, 412.

Holden, J. R. (1962). Naval Ordnance Laboratory report NOLTR 62–46; [(1963). *C. A.* **59**, 13417*h*].

Howells, E. R., Phillips, D. C. & Rogers, D. (1950). *Acta Cryst.* **3**, 210.

Lipson, H. & Cochran, W. (1957). *The Determination of Crystal Structures.* 2nd ed., p. 300, London: Bell.

McWeeny, R. (1951). *Acta Cryst.* **4**, 513.

McWeeny, R. (1952). *Acta Cryst.* **5**, 463.

McWeeny, R. (1953). *Acta Cryst.* **6**, 631.

McWeeny, R. (1954). *Acta Cryst.* **7**, 180.

Pauling, L. (1960). *The Nature of the Chemical Bond.* 3rd ed., chap. 7. Ithaca: Cornell Univ. Press.

Trueblood, K. N. (1962). *I.U.Cr. World List of Crystallographic Computer Programs.* 1st ed., Groningen.

Ramachandran, G. N. & Srinivasan, R. (1959). *Acta Cryst.* **12**, 410.

Acta Cryst. (1965). **18**, 496

The Crystal Structure of the Tetragonal Bronze $Ba_6Ti_2Nb_8O_{30}$

By N. C. Stephenson

School of Inorganic Chemistry, University of New South Wales, Sydney, Australia

(*Received* 14 *April* 1964)

The structure of the tetragonal bronze $Ba_6Ti_2Nb_8O_{30}$ has been determined by single-crystal X-ray analysis. The light-atom positions were determined from three-dimensional Fourier difference synthesis sections and the positional coordinates of all atoms were refined by cycles of differential syntheses. The Ti and Nb atoms are statistically distributed throughout the structure and are each surrounded by an octahedron of oxygen atoms. The metal–oxygen octahedra are joined together by corners in a framework containing four- and five-side tunnels which run through the structure. The barium ions fully occupy all available sites in these tunnels.

The space is *P4bm*. The metal atoms are displaced from the centres of gravity of the surrounding octahedra of oxygen atom. These displacements occur in the same direction resulting in a polar [001] axis, characteristic of a line ferroelectric.

Introduction

The tetragonal tungsten bronze structure was deduced by Magnéli (1949) for the phase K_xWO_3 ($0{\cdot}48 < x < 0{\cdot}54$). In this study, the positions of the tungsten and potassium atoms were found by single-crystal techniques, but the oxygen atoms were placed in positions which afforded a reasonable stereochemical environment and were not confirmed by direct methods.

This structure arises not only in metal oxide 'bronzes' but in materials of high dielectric constant.

Francombe & Lewis (1958) showed that the large orthorhombic cell of lead metaniobate, $PbNb_2O_6$, is similar to that of tetragonal tungsten bronze. The many ferroelectric phases which can be produced by ionic substitution in lead metaniobate have superstructures based upon the tetragonal bronze. Compounds with this structure are usually variable in composition.

The substance $Ba_6Ti_2Nb_8O_{30}$ does not suffer from composition variability and is saturated with respect to metal and oxygen positions. No superstructure, such as a doubling of the c axis, appears in this compound, and in this respect it is unique. The barium bronze is also a ferroelectric and would seem an ideal substance with which to establish, with some degree of accuracy, the positions of the oxygen atoms in the tetragonal bronze structure. This study is to be extended to a detailed examination of related compounds where composition variation and superstructure formation are known to occur.

Experimental

Crystals of $Ba_6Ti_2Nb_8O_{30}$ were prepared at the National Bureau of Standards, Washington, D.C., U.S.A. by the Verneuil flame fusion technique; they are colourless and opaque. They are comparatively brittle and fragment without noticeable cleavage.

An optical examination proved them to be uniaxial with $2V$ equal to zero. The diffraction symbol $4/mmm$ was indicated by the single-crystal X-ray data so that the unit cell is tetragonal. The following unit-cell dimensions were obtained from zero layer precession photographs taken with Mo $K\alpha$ radiation; $a = 12{\cdot}54 \pm 0{\cdot}05$, $c = 4{\cdot}01 \pm 0{\cdot}01$ Å. Evidence for a pseudo-tetragonal cell, such as the splitting of high-angle reflexions, was negative.

The only systematic absences noted in the diffraction data occurred for reflexions $0kl$ with $k = 2n+1$. This is characteristic of the space groups $P4/mbm$ (D^5_{4h}), $P4bm$ (C^2_{4v}) and $P\bar{4}b2$ (D^7_{2d}) in the tetragonal system. A possibility arises that the unit cell is orthorhombic with $a=b$, in which case the space group would be $Pbm2$ or $Pb2_1m$. The latter space group is structurally unsound in view of the short length of the c axis since it requires atoms to be grouped together in pairs, *e.g.* at (x, y, z) and $(z, y, \bar{z})$. The space group $Pbm2$ requires that many vectors between atoms related by the symmetry elements of the space group should be in the planes (100) or (010). This is not consistent with the vector distribution in the ($hk0$) Patterson map (Fig. 1). The structure analysis has thus proceeded on the assumption that $Ba_6Ti_2Nb_8O_{30}$ has a tetragonal unit cell.

Reflexion intensity data were collected from a needle shaped crystal, 0·035 cm in length and with an average cross sectional diameter of 0·007 cm. The c axis of the tetragonal cell was parallel to the needle axis of the crystal and faces of the form (110)

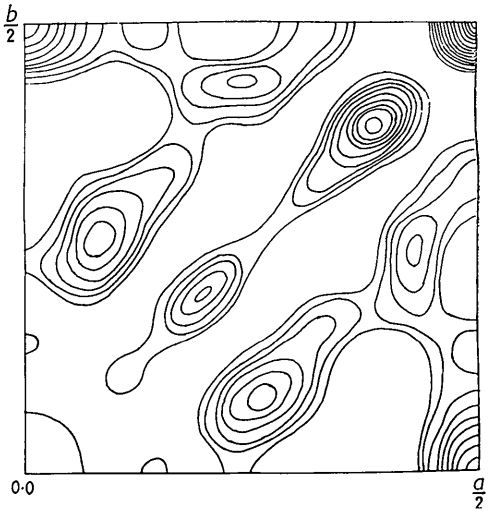

Fig. 1. The Patterson projection along [001] for $Ba_6Ti_2Nb_8O_{30}$.

were prominently developed. Cu $K\alpha$ ($\lambda = 1{\cdot}5407$ Å) radiation and a Weissenberg goniometer were used in equi-inclination geometry. The $hk0$–3 intensity data were recorded by the multiple film technique and measurements made by visual comparison with a standard series of spots recorded in the usual manner. Another crystal was mounted about the [110] axis and used to collect correlation data. This crystal setting also allowed the $hk0$ diffraction data to be collected using zero layer precession photography and Mo $K\alpha$ ($\lambda = 0{\cdot}7107$ Å) radiation. Intensities in this instance were measured photometrically.

The $Ba_6Ti_2Nb_8O_{30}$ intensity data were corrected for Lorentz and polarization effects with the use of a transparent overlay based upon the chart prepared by Waser (1957) for the precession method of recording. The intensity reduction programmes of Sime (1961) for use with the UTECOM digital computer were used for the Weissenberg data.

Atomic form factors for O^- and Ti^{3+}, and for Nb^{4+} and Ba^{2+} were taken from Hartree (1962) and from Thomas & Umeda (1957) respectively. Corrections for the real component of the anomalous dispersion of Cu $K\alpha$ by barium, niobium and titanium were made with the f' value given by Dauben & Templeton (1955).

Structure determination and refinement

A survey of the corrected intensities drew attention to a nearly identical distribution of $hk0$ and $hk2$ intensities. All the atoms comprising the structure are therefore situated in, or very close to, two planes normal to the z axis and $c/2$ Å apart. The space groups $P4/mbm$, $P4bm$ and $P\bar{4}b2$ become identical if the z positional parameter is zero or one half. Although the space group $P4/mbm$ is ruled out by the ferroelectric nature of the material, it can be used in the initial stages of the structure determination since the atoms are expected to be only slightly moved from the (001) and (002) planes.

Table 1. *Atomic parameters for* $Ba_6Ti_2Nb_8O_{30}$

Space group *P4bm*

Atom	Point position	Fractional coordinates x/a	y/b	z/c	Standard deviations (Å) $\sigma(x)$	$\sigma(y)$	$\sigma(z)$	Peak heights (e.Å^{-3}) $\varrho(o)$	$\varrho(c)$	Thermal parameter B (Å^2)
Ba	2(*a*)	0·0000	0·0000	0·9937	0·003	0·003	0·004	122·7	124·1	0·16
Ba	4(*c*)	0·1721	0·6721	0·9839	0·003	0·003	0·005	104·9	112·9	0·40
M*	2(*a*)	0·0000	0·5000	0·4817	0·004	0·004	0·007	77·9	76·5	0·45
M	8(*d*)	0·0748	0·2159	0·4562	0·004	0·004	0·006	83·7	77·8	0·30
O	2(*b*)	0·000	0·500	0·021	0·02	0·02	0·08	21·5	18·5	0·10
O	4(*c*)	0·279	0·779	0·500	0·02	0·02	0·04	16·7	15·1	0·15
O	8(*d*)	0·064	0·218	0·000	0·02	0·02	0·04	27·7	26·9	0·15
O	8(*d*)	0·345	0·007	0·500	0·02	0·02	0·03	22·9	25·6	0·10
O	8(*d*)	0·146	0·066	0·500	0·02	0·02	0·03	11·2	13·6	0·60

* The Ti and Nb atoms occupy the metal positions at random. The symbol M represents ($\frac{1}{5}$ Ti + $\frac{4}{5}$ Nb) as a single scattering unit.

The six barium atoms must be in both fourfold and twofold sites, and one of the latter can be the origin. The Patterson function $P(u, v)$, which will be the same for all three space groups, will therefore contain within it direct evidence of the detailed structure. The coordinates proposed by Magnéli (1949) for the heavy atom positions in the tetragonal potassium tungsten bronze K_xWO_3 satisfactorily explain many of the peaks on $P(u, v)$. They are

2 Ba(1) in 2(*a*): (0, 0, 0) *etc.*
4 Ba(2) in 4(*g*): $(x, \frac{1}{2}+x, 0)$ *etc.*
$x \simeq 0{\cdot}175$
2 Ti in 2(*c*): $(0, \frac{1}{2}, \frac{1}{2})$ *etc.*
8 Nb in 8(*j*): $(x, y, \frac{1}{2})$ *etc.*
$x \simeq 0{\cdot}078$
$y \simeq 0{\cdot}209$.

There was a noticeable improvement in the discrepancy index R when the titanium and niobium atoms were allowed to assume random occupancy of sites 2(*c*) and 8(*j*). The close agreement between observed and calculated peak heights for these atoms (Table 1) has been obtained assuming random occupancy.

The centrosymmetric electron-density projection (Fig. 2), was calculated basing phases upon the contribution of metal atoms in the above positions. The distribution of peaks representing the light oxygen atoms and the number of these atoms to be placed within the unit cell left no doubt that the titanium and niobium atoms were each surrounded by octahedra of oxygen atoms, located in the following positions.

8 O(1) in 8(*j*): $(x, y, \frac{1}{2})$ *etc.*
$x \simeq 0{\cdot}1400$
$y \simeq 0{\cdot}0633$
8 O(2) in 8(*j*): $(x, y, \frac{1}{2})$ *etc.*
$x \simeq 0{\cdot}339$
$y \simeq 0{\cdot}008$
8 O(3) in 8(*i*): $(x, y, 0)$ *etc.*
$x \simeq 0{\cdot}078$
$y \simeq 0{\cdot}209$
4 O(4) in 4(*h*): $(x, \frac{1}{2}+x, \frac{1}{2})$ *etc.*
$x \simeq 0{\cdot}279$
2 O(5) in 2(*d*): $(0, \frac{1}{2}, 0)$ *etc.*

Comparison between F_o and F_c, calculated for all atoms, for the *hk*0 reflexions gave a discrepancy of 14%. A three-dimensional Fourier section at $Z=c/2$ using the coefficients $F_o - F_{\text{metals}}$ (Fig. 3) shows the oxygen atoms more clearly.

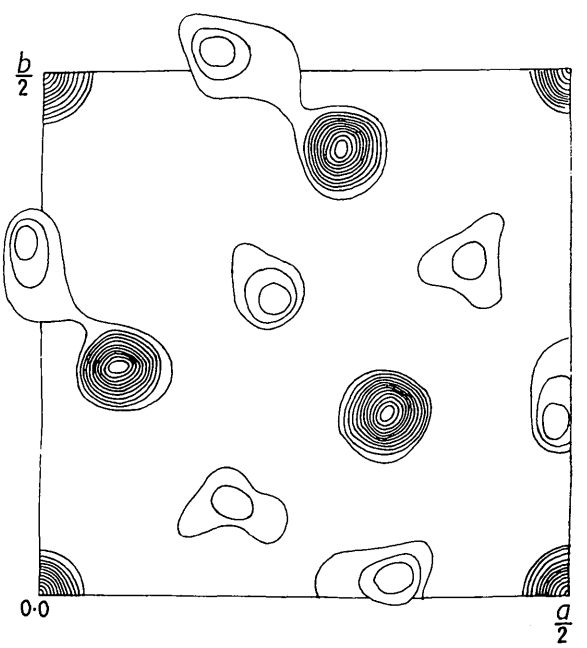

Fig. 2. The centrosymmetric electron-density projection on (001). Phases are based upon the contributions of the heavy metal atoms. Contours drawn on an arbitrary scale.

A choice between the polar space groups *P4bm* and $P\bar{4}b2$ was made by examining the agreement between observed and calculated structure factors when the heavy metal atoms in eightfold position 8(*j*), were arbitrarily displaced from the (002) plane by 0·2 Å. For example, space group *P4/mbm* gave an $R(hk2)$ of 23·7%, $P\bar{4}b2$ gave an $R(hk2)$ of 37·5% and *P4bm* gave an $R(hk2)$ of 21·7% when this new z coordinate was substituted and used with the above listed coordinates to calculate structure factors. This latter space group consistently gave lower values for

the discrepancy index for all data and was therefore accepted as being correct.

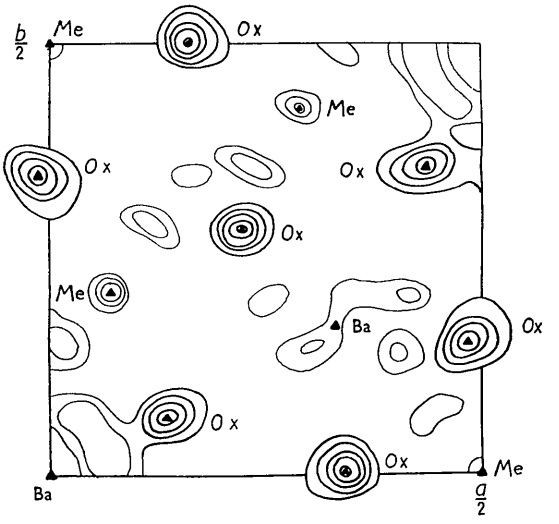

Fig. 3. ($F_o - F_c$) difference Fourier section $z = 0{\cdot}5$, F_c from metal atom contributions only. This section shows high maxima (heavily marked) for the oxygen atoms lying in the plane $z = 0{\cdot}5$ and other ripples and artifacts arising from thermal anisotropy, absorption errors and data termination. Contours at intervals of 4 e.Å^{-3}; zero and negative contours omitted.

A refinement of the positional parameters of all atoms was attempted with successive cycles of differential syntheses and structure factors. The programs of Sime (1961) were used and calculations carried out on the UTECOM digital computer. Isotropic temperature factors for individual atoms were adjusted after each cycle so as to improve the agreement between observed and calculated peak curvatures and the refinement was carried out in the space group *P4bm*. The final parameters and their standard deviations are given in Table 1. These parameters were used to calculate the final set of structure factors which are listed for comparison with F(obs) in Table 2. Many of the observed intensities (*e.g.* 140, 061, 121) suffer badly from extinction and these effects are reflected in low atomic temperature parameters. Several other possible reasons for the temperature factor anomalies may be proposed. The first is an interaction between parameters during the refinement. Unfortunately, the full correlation matrix could not be computed and the extent of parameter interaction is not known. However, the rather abrupt termination of data along the z direction owing to the very short length of the c axis undoubtedly has lead to considerable uncertainty in the z atomic coordinates. The standard deviations listed in Table 1 reflect his uncertainty but the significance of these errors is doubtful.

Another reason could be an incorrect anomalous dispersion correction. The imaginary components of the anomalous dispersion correction were not introduced because the intensities of equivalent reflexions with unlike signs of l appeared to be the same. If the crystal studied contains domains oppositely oriented with respect to C then $I(hkl)$ and $I(hk\bar{l})$ may be superimposed for each reflexion. Yakel, Kochler, Bertaut & Forrat (1963) suggest that in this case $F^2(hkl)$ and $F^2(hk\bar{l})$ should be computed (with imaginary anomalous dispersion corrections) and averaged before comparison with the observed $F^2(hk|l|)$. This procedure was not pursued in view of other intensity errors such as absorption and extinction which had not been corrected.

Stereochemical plausibility, agreement between observed and calculated peak heights, and the appearance of the difference sections all suggest that the proposed structure is correct. Some reflections are drastically affected by primary extinction. This effect is most pronounced under conditions of low Bragg angle scattering and large structure amplitudes. Reflexions suffering from primary extinction are listed in Table 2 with an asterisk. The overall reliability index, which was calculated giving one half the minimum observable intensity to the unobserved reflexions, and omitting data affected by primary extinction, is 0·16. With the above reservations, the structure is now sufficiently established to justify description. The standard deviations average at 0·03 Å for the metal–oxygen distances and 0·04 Å for oxygen–oxygen.

Discussion

The structure of $Ba_6Ti_2Nb_8O_{30}$ is illustrated in Fig. 4. The titanium and niobium metal atoms are disordered, and ($\frac{1}{5}$Ti + $\frac{4}{5}$Nb) represents the average population of metal atom (M) positions in octahedral environ-

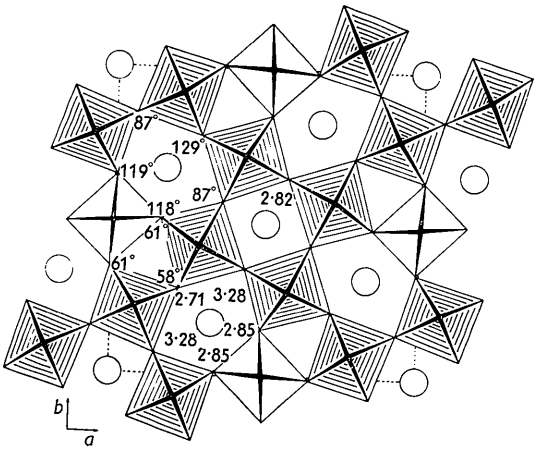

Fig. 4. A drawing of the structure projected along [001] showing the mode of linking of the M–oxygen octahedra and the environment of the barium ions. The irregular octahedra centred on M(8*d*) are shaded. Bond lengths: the standard deviation in metal–oxygen distances is 0·03 Å and in oxygen–oxygen distances, 0·04 Å. Bond angles: the standard deviation is 4°.

Table 2. *Structure factors for* $Ba_6Ti_2Nb_8O_{30}$

Columns show h, k, $|F_c|$, $|F_o|$

l = 0				
0	2	12	22	
0	4	185	163	
0	6	175	181	
0	8	63	51	
0	10	131	128	
0	12	194	167	
0	14	162	159	
1	1	8	12	
1	2	61	43	
1	3	29	10	
1	4	351	278	*
1	5	36	38	
1	6	57	36	
1	7	151	153	
1	8	82	103	
1	9	151	133	
1	10	4	80	
1	11	75	68	
1	12	65	61	
1	13	38	50	
1	14	46	26	
1	15	65	54	
2	3	160	163	
2	4	247	266	
2	5	110	121	
2	6	156	138	
2	7	124	118	
2	8	267	229	
2	9	35	28	
2	10	140	133	
2	11	134	130	
2	12	43	43	
2	13	132	128	
2	14	104	113	
2	15	65	82	
3	3	154	136	
3	4	33	26	
3	5	217	183	
3	6	133	154	
3	7	96	109	
3	8	139	159	
3	9	27	29	
3	10	8	30	
3	11	81	61	
3	12	82	74	
3	13	10	28	
3	14	14	25	
3	15	80	78	
4	4	108	135	
4	5	30	30	
4	6	13	33	
4	7	107	108	
4	8	93	116	
4	9	123	130	
4	10	78	86	
4	11	57	43	
4	12	107	103	
4	13	8	27	
4	14	137	145	
4	15	59	50	
5	5	195	198	
5	6	60	25	
5	7	30	45	
5	8	125	106	
5	9	11	42	
5	10	181	145	
5	11	35	63	
5	12	48	29	
5	13	38	37	
5	14	34	27	
5	15	104	91	
6	6	335	317	
6	7	17	28	
6	8	69	88	
6	9	68	68	
6	10	38	51	
6	11	101	120	
6	12	212	210	
6	13	18	25	
6	14	64	56	
6	15	41	61	
7	7	162	170	
7	8	91	87	
7	9	21	11	
7	10	111	111	
7	11	9	29	
7	12	17	26	
7	13	82	78	
7	14	46	54	
8	8	178	168	
8	9	36	30	
8	10	63	74	
8	11	48	78	
8	12	69	74	
8	13	53	20	
9	9	147	139	
9	10	47	64	
9	11	148	116	
9	12	6	21	
9	13	58	66	
10	10	68	80	
10	11	47	62	
10	12	89	78	
11	11	70	53	
l = 1				
0	2	20	26	
0	4	73	49	
0	6	264	164	*
0	8	15	24	
0	10	41	28	
0	12	109	97	
0	14	178	221	
1	1	95	33	*
1	2	185	100	*
1	3	257	135	*
1	4	29	54	
1	5	43	47	
1	6	9	20	
1	7	200	140	
1	8	77	60	
1	9	104	87	
1	10	211	127	*
1	11	81	94	
1	12	24	28	
1	13	61	69	
1	14	54	68	
1	15	93	107	
2	2	193	113	*
2	3	114	79	
2	4	55	62	
2	5	98	52	
2	6	126	103	
2	7	113	88	*
2	8	47	35	
2	9	29	53	
2	10	42	56	
2	11	11	28	
2	12	44	73	
2	13	37	26	
2	14	86	89	
2	15	19	17	
3	3	60	42	
3	4	6	18	
3	5	149	108	
3	6	87	111	
3	7	117	102	
3	8	92	113	
3	9	69	66	
3	10	20	28	
3	11	191	163	
3	12	47	87	
3	13	117	149	
3	14	27	53	
3	15	10	66	
4	4	115	93	
4	5	197	168	
4	6	26	22	
4	7	137	117	
4	8	103	113	
4	9	41	67	
4	10	58	49	
4	11	69	69	
4	12	58	66	
4	13	140	133	
4	14	32	58	
4	15	130	105	
5	5	175	166	
5	6	66	71	
5	7	92	102	
5	8	36	27	
5	9	216	206	
5	10	21	28	
5	11	38	28	
5	12	14	58	
5	13	48	57	
5	14	29	19	
6	6	91	101	
6	7	42	27	
6	8	89	78	
6	9	47	80	
6	10	44	63	
6	11	51	81	
6	12	64	61	
6	13	15	21	
6	14	12	57	
7	7	40	39	
7	8	57	75	
7	9	141	145	
7	10	80	73	
7	11	67	58	
7	12	26	33	
7	13	148	172	
7	14	40	37	
8	8	65	75	
8	9	71	97	
8	10	70	109	
8	11	113	139	
8	12	69	87	
8	13	76	77	
9	9	31	100	
9	10	93	111	
9	11	84	93	
9	12	26	40	
10	10	36	22	
10	11	54	62	
11	11	58	99	
l = 2				
0	2	24	13	
0	4	133	82	*
0	6	157	118	*
0	8	61	50	
0	10	113	108	
0	12	175	157	
0	14	142	203	
1	1	12	19	
1	2	56	30	
1	3	48	34	
1	5	33	22	
1	6	45	33	
1	7	121	94	
1	8	72	74	
1	9	130	97	
1	10	36	38	
1	11	65	68	
1	12	57	64	
1	13	35	56	
1	14	42	20	
2	2	74	39	*
2	3	105	81	
2	4	198	129	*
2	5	91	86	
2	6	122	106	
2	7	105	73	
2	8	209	150	
2	9	31	22	
2	10	121	117	
2	11	118	122	
2	12	50	49	
2	13	118	132	
2	14	97	95	
3	3	123	107	
3	4	25	16	
3	5	176	153	
3	6	110	121	
3	7	83	96	
3	8	121	136	
3	9	28	22	
3	10	8	22	
3	11	77	60	
3	12	74	73	
3	13	18	41	
3	14	14	13	
4	4	95	86	
4	5	29	31	
4	6	27	27	
4	7	94	83	
4	8	87	106	
4	9	107	117	
4	10	71	76	
4	11	51	55	
4	12	95	133	
4	13	21	28	
4	14	125	120	
5	5	158	146	
5	6	33	35	
5	7	25	41	
5	8	107	85	
5	9	29	49	
5	10	159	152	
5	11	32	85	
5	12	40	36	
5	13	36	44	
5	14	32	8	
6	6	284	237	*
6	7	15	22	
6	8	58	72	
6	9	60	56	
6	10	41	44	
6	11	90	141	
6	12	207	226	
7	7	144	171	
7	8	81	90	
7	9	28	42	
7	10	101	95	
7	11	8	18	
7	12	34	26	
7	13	74	57	
8	8	158	151	
8	9	33	20	
8	10	61	99	
8	11	48	106	
8	12	61	90	
9	9	131	127	
9	10	45	98	
9	11	134	141	
10	10	63	73	
l = 3				
0	2	19	27	
0	4	56	57	
0	6	196	147	*
0	8	28	18	
0	10	40	49	
0	12	91	139	
1	1	69	28	
1	2	127	104	
1	3	181	141	*
1	4	56	48	
1	5	48	27	
1	6	2	17	
1	7	149	129	
1	8	60	48	
1	9	94	83	
1	10	165	140	
1	11	66	96	
1	12	24	13	
1	13	59	46	
2	2	131	111	
2	3	87	82	
2	4	99	99	
2	5	71	46	
2	6	96	84	
2	7	86	76	
2	8	55	55	
2	9	23	49	
2	10	44	66	
2	11	32	34	
2	12	39	64	
3	3	33	41	
3	4	6	16	
3	5	123	94	
3	6	78	88	
3	7	97	85	
3	8	82	109	
3	9	90	61	
3	10	16	17	
3	11	155	149	
3	12	47	77	
4	4	77	77	
4	5	145	132	
4	6	16	18	
4	7	105	93	
4	8	78	101	
4	9	42	65	
4	10	46	52	
4	11	56	58	
4	12	55	53	
5	5	130	143	
5	6	50	58	
5	7	73	78	
5	8	32	16	
5	9	158	139	
5	10	40	22	
5	11	37	13	
5	12	13	34	
6	6	82	93	
6	7	32	18	
6	8	73	74	
6	9	40	68	
6	10	33	53	
6	11	48	59	
7	7	81	58	
7	8	47	63	
7	9	114	126	
7	10	68	59	
7	11	56	34	
8	8	57	67	
8	9	57	79	
8	10	55	79	
9	9	32	70	

ment. The lattice is constructed of MO_6 octahedra joined by corners, every oxygen atom thus being common to two M atoms. This agrees with the atomic ratio 3:1 of these two species of atoms. Parallel to [001] the octahedra are linked together to form long chains so that each octahedron in Fig. 4 represents an infinite chain extending along the axis of projection. Parallel to (001) the octahedra are coupled together in an intricate way forming rings of three, four or five octahedra. The Ba ions are situated in the interstices between adjacent tetragons and pentagons. Each Ba(2*a*) atom, exhibiting eightfold coordination, is surrounded regularly by oxygen atoms, each with a Ba–O separation distance of 2·82 Å. This distance agrees well with a normal ionic separation of 2·75 Å (Pauling, 1960) and the radius ratio of 0·96 would predict a coordination number in excess of eight for the barium–oxygen system. The Ba(4*c*) ions are surrounded at various distances by ten oxygen atoms, six of them at distances of 2·71–2·85 Å and the remaining four at remote distances of 3·28 Å.

The octahedron centred upon M(2*a*) is more regular than the M(8*d*) octahedron. The interionic contacts for each of these octahedra are depicted in Fig. 5. The average M–O distances in the above octahedra are 1·96 and 2·00 Å respectively and these compare favourably with data given by Wadsley (1961) for these metal–anion distances. The O–O approach distances do not significantly differ from that expected for normal anionic contact. The shortest distances (3·69–3·71 Å) between M atoms occurs when the octahedra associated with these atoms share corners so that they encompass a triangle (*cf.* Fig. 4).

The M(2*a*) and M(8*d*) atoms are displaced from the (002) plane by distances of 0·08 and 0·17 Å respectively. These displacements from the centres of gravity of the surrounding octahedra of oxygen atoms are significant ($\Delta/\sigma = 11$ and 30) and occur in the same direction. The substance should therefore possess the characteristics of a line ferroelectric. The angles subtended at M(2*a*) and M(8*d*) by oxygen atoms which are diagonally opposite one another in the (002) plane are 176° and 169° (average) respectively.

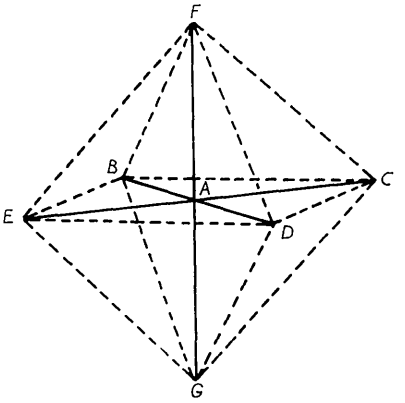

Fig. 5. The approximate ionic arrangement in the two different type of octahedral groupings of oxygen ions around M ions. Standard deviations in bond distances and angles as in Fig. 4.

Bond	*d*(irreg.)	*d*(reg.)	Bond	*d*(irreg.)	*d*(reg.)
A–B	1·93 Å	1·94 Å	*B–G*	2·71 Å	2·73 Å
A–C	2·01	1·94	*C–D*	2·83	2·62
A–D	2·09	1·94	*C–F*	2·92	2·85
A–E	1·98	1·94	*C–G*	2·92	2·73
A–F	2·18	2·16	*D–E*	2·84	2·86
A–G	1·84	1·85	*D–F*	2·95	2·85
B–C	2·97	2·86	*D–G*	2·95	2·73
B–E	2·61	2·62	*E–F*	2·74	2·85
B–F	2·72	2·85	*E–G*	2·74	2·73

Angle	Irreg.	Reg.	Angle	Irreg.	Reg.
BAE	83·9°	85·0°	*CAD*	87·6°	85·0°
BAC	98·3	94·9	*CBE*	90·3	90·0
BCD	86·7	90·0	*CDE*	88·9	90·0
BED	94·1	90·0	*DAE*	88·4	94·9

The author would like to thank Dr A. D. Wadsley for introducing him to solid state chemistry and for many valuable discussions. He is also indebted to Dr R. S. Roth of the National Bureau of Standards, Washington, for providing the single crystals.

References

Dauben, C. H. & Templeton, D. H. (1955). *Acta Cryst.* **8**, 841.

Francombe, M. H. & Lewis, B. (1958). *Acta Cryst.* **11**, 696.

Hartree, D. R. (1962). *International Tables for X-ray Crystallography*. Vol. III, Section 3·3·1.

Magnéli, A. (1949). *Ark. Kemi*, **1**, 213.

Pauling, L. (1960). *The Nature of the Chemical Bond.* 3rd ed. Ithaca: Cornell Univ. Press.

Sime, J. (1961). *Computing Methods and the Phase Problem in X-ray Crystal Analysis*. Oxford: Pergamon Press.

Thomas, L. H. & Umeda, K. (1957). *J. Chem. Phys.* **26**, 293.

Wadsley, A. D. (1961). *Acta Cryst.* **14**, 660.

Waser, J. (1957). *Rev. Sci. Instrum.* **22**, 567.

Yakel, H. L., Kochler, W. C., Bertaut, E. F. & Forrat, E. F. (1963). *Acta Cryst.* **16**, 957.